Progress In Electromagnetics Research C, Vol. 125, 229–240, 2022

Design and Analysis of a Bandwidth Enhanced Low-Profile SIW Cavity-Backed Slot Antenna Using TE_{210} Mode

Bollavathi Lokeshwar[1, *], Jammalamadugu Ravindranadh[1], and Devabhaktuni Madhavi[2]

Abstract—In this paper, a bandwidth improvement technique in SIW slotted antennas is presented. Distinct from conventional SIW antennas with multiple cavity modes, a single cavity mode (TE_{210}) is utilized to improve the bandwidth. When a rectangle slot is loaded at bottom surface of the cavity, the TE_{210} cavity mode is perturbed. As a result, two independent modes (odd TE_{210}, even TE_{210}) are introduced and merged in close proximity. Finally, the antenna is fabricated and tested. The measured results render an impedance bandwidth of 12.8% and a maximum gain of 7.1 dBi. The cross-polar level of maximum −29 dB and −34 dB is at 9.73 GHz and 10.63 GHz, respectively. The proposed design holds many features such as easy fabrication and light weight. Besides, the proposed design is single-layered that makes it extremely convenient to integrate with other planar configurations.

1. INTRODUCTION

Due to the rapid proliferation of wireless commination technology, there is an urgent need of high-performance and low-profile antennas providing compatibility with planar circuits. Micro-strip antenna possesses a bidirectional pattern with light weight, easy fabrication, and easy integration [1–3]. Traditional cavity-backed antennas render low back radiation, low loss, and high gain. However, the integration with planar geometry is a daunting task due to large size and heavy weight [4, 5].

A new concept is reported by Deslandes and Wu with the innovation of substrate integrated waveguide (SIW) [6]. SIW implements the conventional cavity-backed antennas in planar form [7]. The outstanding features of SIW are the high-density integration with conventional planar components (e.g., microstrip lines and coplanar waveguides), the easy manufacturing, and the low power losses [8–11]. This SIW is still in a development phase in the design of microwave and millimeter-wave components. Several planar slot antennas have been reported in the literature on the basis of SIW technology. Albeit benefits like low losses, easy integration, and easy fabrication, they offer narrow bandwidth due to a thin substrate. The first printed slot antenna on the basis of SIW technique is described in [12], which generates the radiation by TE_{120} mode of the cavity at 10 GHz. Due to high quality factor (Q), the bandwidth achieves only 1.7% with a gain of 5.3 dBi.

In [13], the bandwidth of 6.3% is obtained by combining the two hybrid modes of the cavity in close proximity. In [14], an offset feeding method is used to excite the TE_{120} mode, which results in an impedance bandwidth of 4.2%. In [15], two cavity modes TE_{110} and TE_{120} are perturbed by using a modified bow-tie slot. As a result, it has achieved a bandwidth up to 9.4%. In [16], a method of corner perturbation in the square cavity enhances the bandwidth (1.65%). In [17], a matching slot excites the TE_{210} mode to attain the bandwidth up to 8%. In [18], multi-resonant slots have achieved a bandwidth up to 11%. The design of a wideband SIW antenna is presented in [19], where degenerate modes (TE_{120}

Received 17 August 2022, Accepted 18 October 2022, Scheduled 25 October 2022

* Corresponding author: Bollavathi Lokeshwar (lokesh5701@gmail.com).

[1] Department of ECE, R.V.R & J.C College of Engineering, Guntur, India. [2] Department of Physics, R.V.R & J.C College of Engineering, Guntur, India.

and TE_{210}) of the cavity are significantly coupled by cutting the edges of the cavity with a circular structure. However, impedance bandwidth enhancement does not surpass 5.7% in this design.

In [20], bandwidth is improved by exciting the TM_{010} mode of the patch using a half-mode SIW cavity. This design shows 10% impedance bandwidth. In [21], a novel wideband hexagonal cavity-backed slot antenna is discussed, where the antenna has achieved the −10 dB bandwidth of 14%. Several bandwidth enhanced cavity-backed antennas are obtained by using bilateral slots [22], butterfly-shaped slot with SIW circular cavity [23], a bow-tie shaped slot [24], stacked cavities [25], loading two metallic posts near the slots [26], spiral-shaped patch [27], E-shaped patch [28], I-shaped slot [29, 30], rectangular slot with shorting vias [31], and crossed-slot with shorting vias [32].

In this paper, bandwidth is improved by perturbing a TE_{210} mode instead of multiple modes as compared to the methods reported in [12–32]. This novel approach is a more distinct method than the other cavity-backed SIW antennas. With the proper arrangement of SIW cavity, microstrip line, and radiating slot, the current density of TE_{210} mode is perturbed. As a result, two independent modes are generated. The wide bandwidth of 1.25 GHz (12.4%), lying between 9.45 GHz and 10.7 GHz, is obtained by merging the resonant frequencies of these modes. Circuit models are developed for the children's TE_{210} mode, and it is substantiated by full-wave simulations. The antenna design is presented in Section 2, followed by the working principle. A parametric study is discussed in Section 4. Section 5 enlightens the discussion of simulated and measured results. The conclusions are presented in Section 6.

2. ANTENNA GEOMETRY AND DESIGN STEPS

Figure 1 depicts the configuration of the proposed antenna, which mainly comprises a dielectric substrate, SIW cavity, radiating slot and feeding element. The entire antenna is designed on RT/duroid 5880 dielectric material ($\varepsilon_r = 2.2$, $\tan\delta = 0.0009$). It begins with the microstrip line fed SIW cavity and followed by rectangle slot loading. The SIW cavity is fabricated by printed circuit board (PCB) processe, where cavity side walls are set up by drilling multiple plated through holes along the edges of the substrate. To emulate the conventional cavity, the pitch (p) and post diameter (d) must follow the conditions $d/p \geq 0.5$ and $d/\lambda_0 \leq 0.1$ to reduce the power losses [33]. The Ansoft HFSS is utilized to design the proposed antenna. The antenna dimensions are initially derived from Equations (1)–(3).

$$f_{mnp'} = \frac{1}{2\sqrt{\mu_0\varepsilon_0\varepsilon_r}}\sqrt{\left(\frac{m}{L_{eff}}\right)^2 + \left(\frac{n}{W_{eff}}\right)^2 + \left(\frac{p'}{h}\right)^2} \tag{1}$$

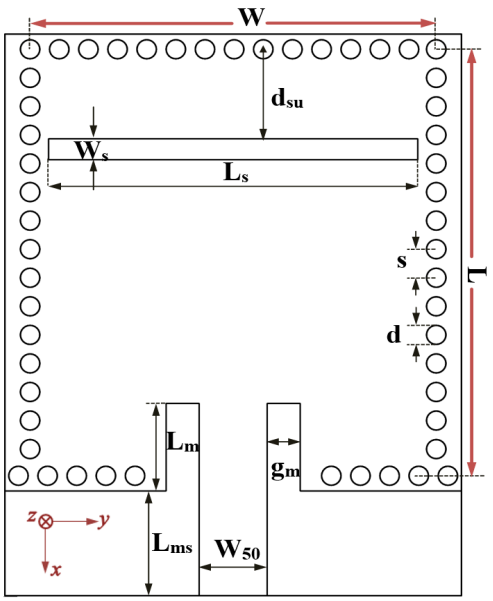

Figure 1. Configuration of the antenna.

$$L_{eff} = L - \frac{d^2}{0.95 * s} \tag{2}$$

$$W_{eff} = W - \frac{d^2}{0.95 * s} \tag{3}$$

where m, n, and p' are numbers of half-cycles in x, y, and z directions, respectively; cavity equivalent length is L_{eff} and width W_{eff}; ε_r is the dielectric constant; d is the via diameter; s is the pitch.

The size of the slot $L_s \times W_s$ is printed on bottom SIW surface. The initial length of the rectangle slot is calculated as 17.4 mm by using the formula as given in Equation (4). A 50 Ω microstrip line is used to excite the modes of the cavity.

$$L_s = \frac{c}{2f_1\sqrt{\varepsilon_{eff}}}; \quad \varepsilon_{eff} = (\varepsilon_r + 1)/2 \tag{4}$$

where l_s is the slot length, ε_{eff} the equivalent permittivity, c the speed of light, and f_1 the resonant frequency of the TE_{110} mode.

The following steps are considered for designing the proposed antenna.

Step1: Select substrate: RT/duroid 5880 ($h = 1.6$ mm, $\varepsilon_r = 2.2$).

Step2: Construct SIW cavity: Rectangular SIW cavity.

Step3: Study and identify the modes of the cavity.

Step4: Place the slot on the cavity to translate the cavity resonator into a slotted radiator.

Step5: Optimize the location and size of the slot, also the dimensions of the feed line.

Step6: Simulate the antenna on HFSS platform. The dimensions are listed in Table 1.

Table 1. Dimensions of the projected SIW antenna.

Parameter	Value (mm)	Parameter	Value (mm)
W	20.9	L_m	4.6
L	22.4	g_m	1.25
s	1.5	W_s	1.4
d	1	d_{su}	4.55
W_{50}	3.3	h	1.6
L_{ms}	5.5		

3. WORKING MECHANISM

3.1. Discussion on the Transverse Electric Mode

In order to perceive the antenna working mechanism, the simulation of the SIW cavity is described first. Figure 2 shows the input resistance curve ($\mathrm{Re}(Z_{11})$), which certifies the wideband impedance matching properties and is also used for recognizing the modes of the cavity. When the SIW cavity is fed by a microstrip feedline, the TE_{110} (fundamental resonance) at 6.8 GHz and TE_{210} (higher order resonance) at 10.2 GHz are excited simultaneously. For the TE_{110} and TE_{210} modes of the SIW cavity, the E-field direction is normal to the top and bottom conductive surfaces while the H-field direction is parallel to the top and bottom conductive layers. Figures 3(a)–(b) illustrate the distributions of the E-field in the cavity for the TE_{110} and TE_{210} modes.

The introduced non-resonant slot perturbs the cavity mode. Hence, the TE_{110} mode is moved to 6.1 GHz from 6.8 GHz. Apart from that, two higher order modes at 9.55 and 10.85 GHz are generated due to perturbations in TE_{210} mode. Figures 4(a)–(c) depict magnitude distributions of the E-field in the cavity with a slot. These modes are merged together by placing the slot at optimum location, which widens the bandwidth. The vector E-field profiles of the antenna at 9.75 GHz and 10.5 GHz are shown in Figure 5. It is observed that the field is mainly concentrated around the applied slot. The absolute E-fields at two sides of the slot are different, which in turn helps the slot to radiate into the air.

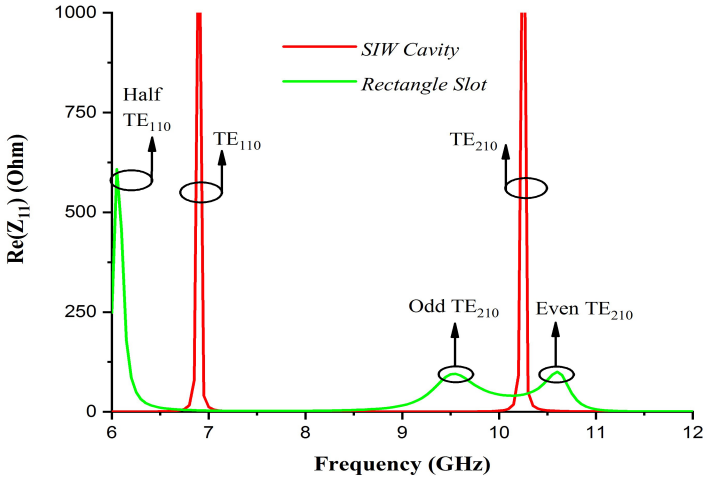

Figure 2. Real input impedance (Z_{11}).

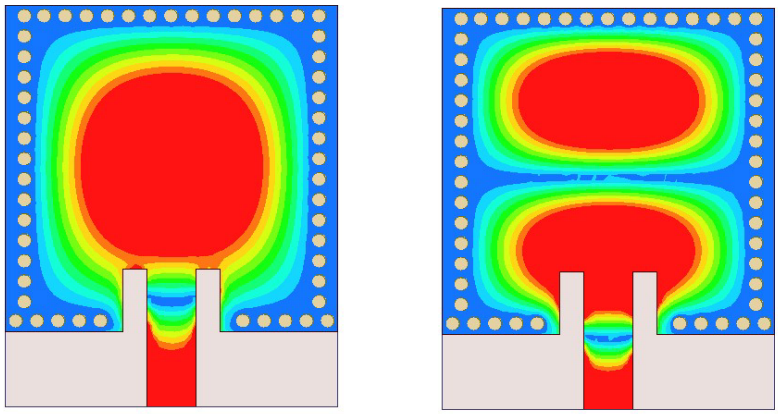

(a) TE_{110} (b) TE_{210} mode

Figure 3. Electric field distributions of SIW cavity.

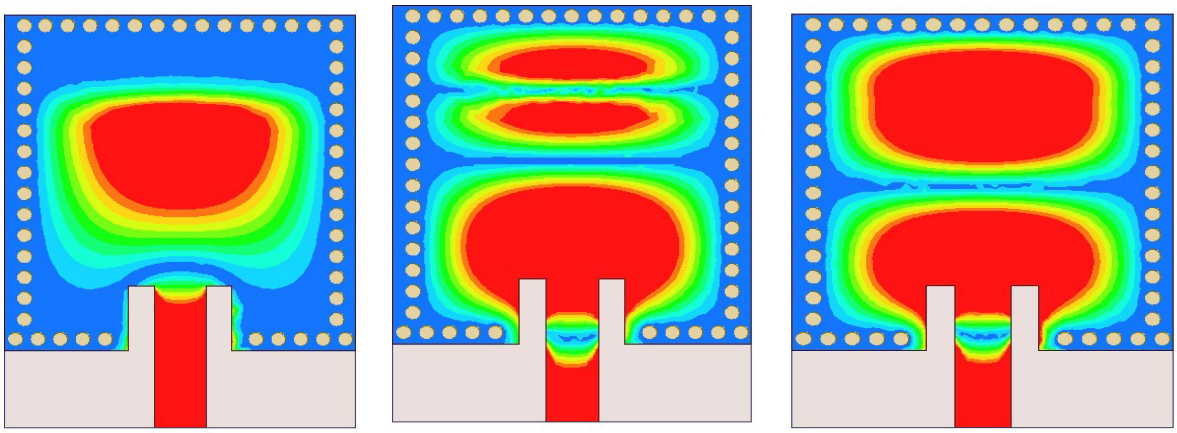

(a) half TE_{110} mode (b) odd TE_{210} mode (c) even TE_{210} mode

Figure 4. Distribution of E-field across the rectangle slot.

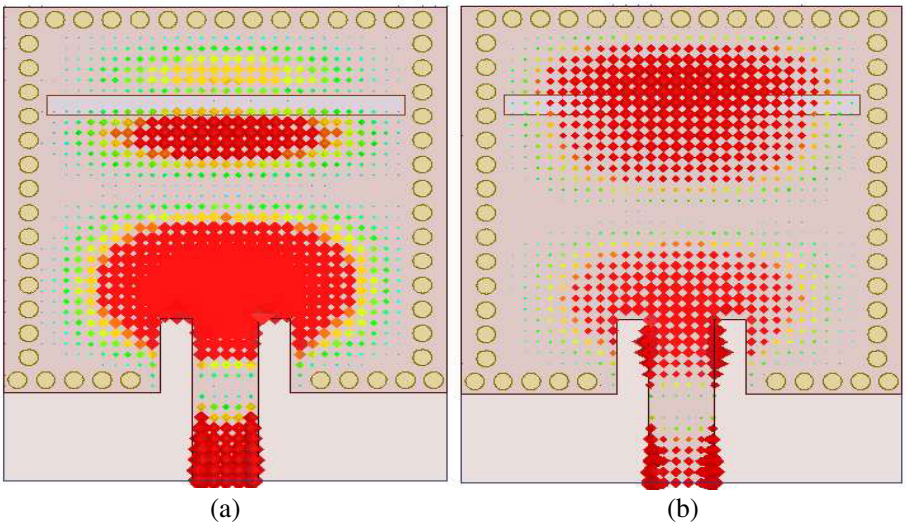

Figure 5. *E*-field vector at (a) odd TE_{210}, (b) even TE_{210}.

3.2. Circuit Models of the Transverse Electric Modes

To provide a deep understanding of the proposed antenna with more intuition, an approximate analysis with the help of equivalent circuit models for the odd TE_{210} and even TE_{210} is given in this section. Note that the circuit models do not include the microstrip line feeding to make the analysis simple. To develop the circuit model for the designed structure operating in TE_{210} mode, first consider the slot impedance which can be represented as a parallel combination of C_s, the capacitance of the non-resonant slot, and R_r, radiation effect of the slot. Moreover, the two ends of the cavity can be terminated by a short circuit since the cavity walls are assumed to be electric walls. The equivalent cavity model of TE_{210} mode is shown in Figure 6, which is bounded by four electric walls at four sides.

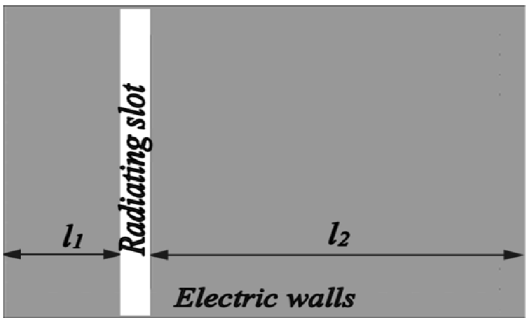

Figure 6. Simplified cavity model of TE_{210} mode.

Figures 7(a)–(c) represent the simplified circuit models for the TE_{210} mode and its children's. For the odd TE_{210} mode, the voltages at both sides of the slot are out of phase. Therefore, the equivalent circuit of the TE_{210} mode can be divided into two half circuits as shown in Figures 7(b) & (c), where each half circuit is a parallel combination of $2C_s$ and $R_s/2$. Thereby, the circuit is loaded with capacitance C_s and resistance R_r. For the even TE_{210} mode, the circuit model can be drawn by considering no loading effect of the slot since the voltage at two sides of the slot are equal.

From the above theoretical analysis, it can be concluded that, due to the capacitive loading in the odd TE_{210} mode, the resonant frequency is lower than even TE_{210} mode. As C_s increases, resonant frequency decreases.

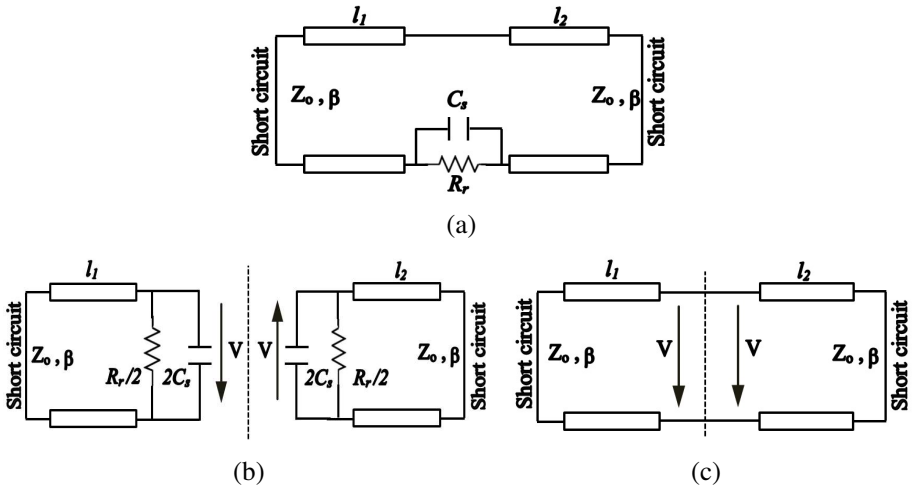

Figure 7. Simplified circuit models of TE modes (a) TE_{210}, (b) odd TE_{210}, and (c) even TE_{210}.

4. PARAMETRIC STUDY

To verify the mechanism of the antenna with better understanding, an extensive parametric test is conducted using HFSS solver. Here, some critical parameters of the final design are varied. That is, during parametric analysis, a particular parameter is varied while all the parameters are kept constant.

4.1. Analysis of Width of Slot "W_s"

When the slot width W_s is changed as shown in Figure 8(a), the impedance matching properties are greatly affected. However, by adjusting the W_s the desired impedance bandwidth can be attained. At optimum $W_s = 1.4$ mm, the maximum bandwidth was obtained. Mathematically, fractional (percentage) bandwidth is calculated from Equation (5). The gain of the antenna is shown in Figure 8(b) for various values of W_s. It is observed that the gain of the antenna is increased as the width W_s increases. It is

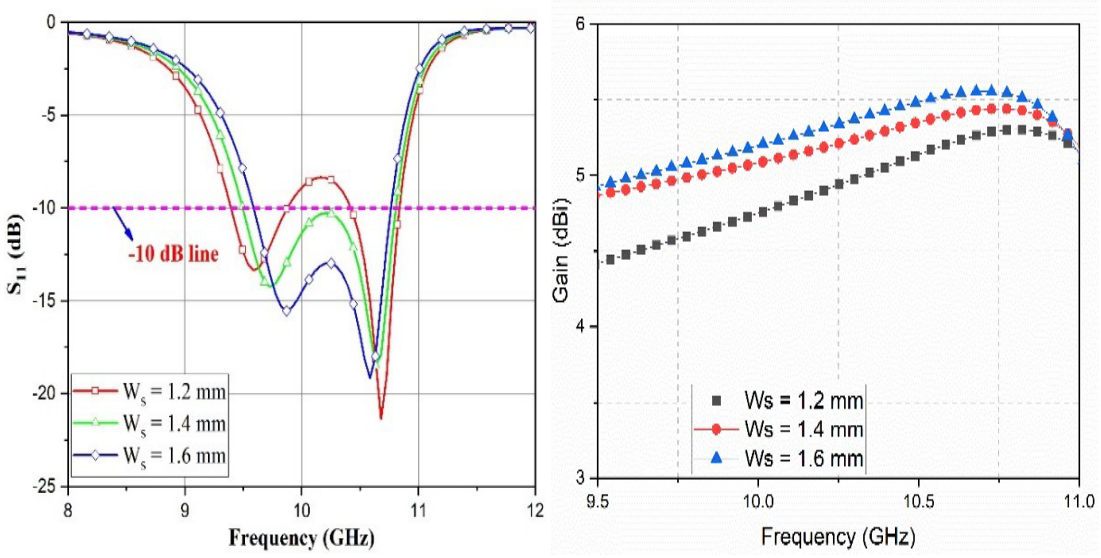

Figure 8. (a) Simulated S_{11}, (b) simulated gain for different values of slot width (W_s).

also verified from the gain expression (6).

$$\%\ Fractional\ Bandwidth = 2 \times \frac{f_H - f_L}{f_H + f_L} \times 100\% \tag{5}$$

where f_L — lower -10 dB frequency; f_H — upper -10 dB frequency

$$G = \frac{4\pi}{\lambda^2} \varepsilon_{ap} A_p \tag{6}$$

4.2. Analysis of Length of Slot "L_s"

Figure 9 shows the impact of slot length on S-parameter of the antenna. It is found that slot length has negligible influence on its center operating frequency. However, a significant effect on S_{11} has been noticed. Hence, it is an important dimension to adjust the antenna's reflection coefficient.

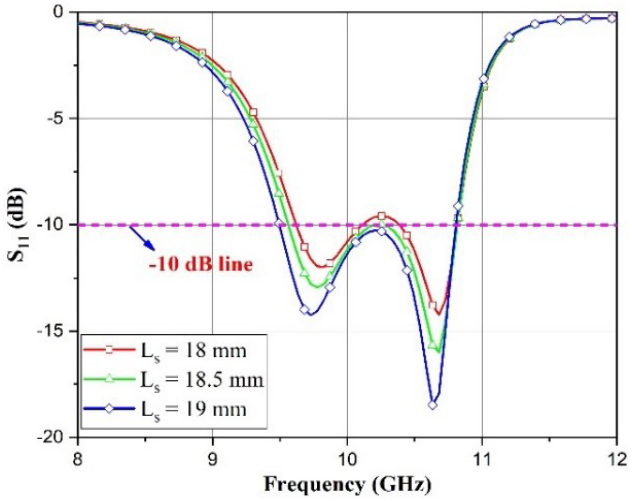

Figure 9. S_{11} for various slot length (L_s).

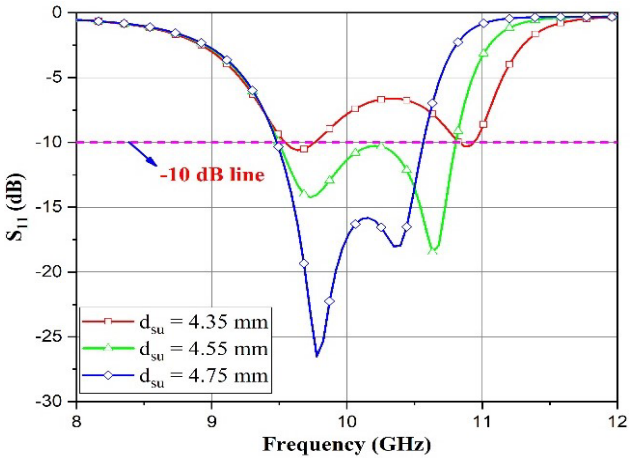

Figure 10. S_{11} for different values of slot position d_{su}.

4.3. Analysis of Position of Slot "d_{su}"

As shown in Figure 10, the variation in the slot position d_{su} from 4.35 mm to 4.75 mm in step size of 0.2 mm leads to disturbance in the current path, and thereby, S_{11} of the antenna is improved. When $d_{su} = 4.35$ mm, the S_{11} value is more than -10 dB. So, the antenna suffers from impedance matching. When $d_{su} = 4.55$ mm, the antenna has good S_{11} value, i.e., less than -10 dB and good bandwidth. However, when $d_{su} = 4.75$ mm, it can be seen that upper resonance is shifted toward the lower frequency. Thus, the optimum value of the slot position is selected as 4.55 mm.

4.4. Analysis of Thickness of Substrate "h"

Figure 11 shows the magnitude of reflection coefficients of different substrate thickness variations. When the height increases, the bandwidth is enhanced up to 12.4%. The figure shows that the substrate thickness of 1.6 mm provides a wide bandwidth and low return loss.

5. RESULTS AND DISCUSSION

To verify the proposed antenna, a prototype is fabricated and tested. The antenna prototype fed by the microstrip line is shown in the inset of Figure 12. The reflection coefficient (S_{11}) is measured by

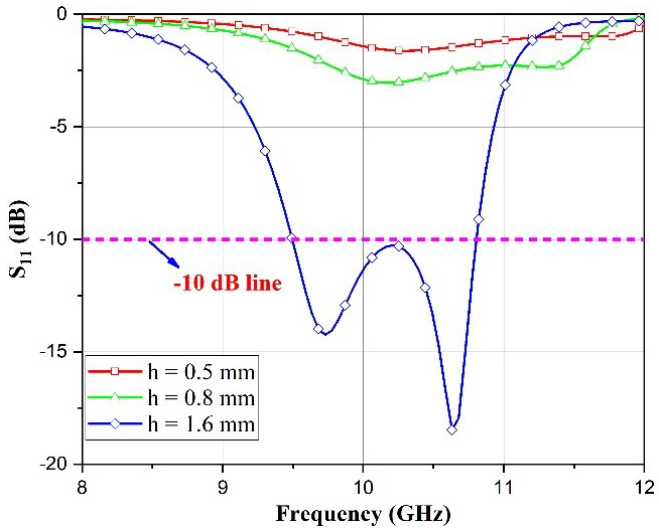

Figure 11. S_{11} for different values of substrate height h.

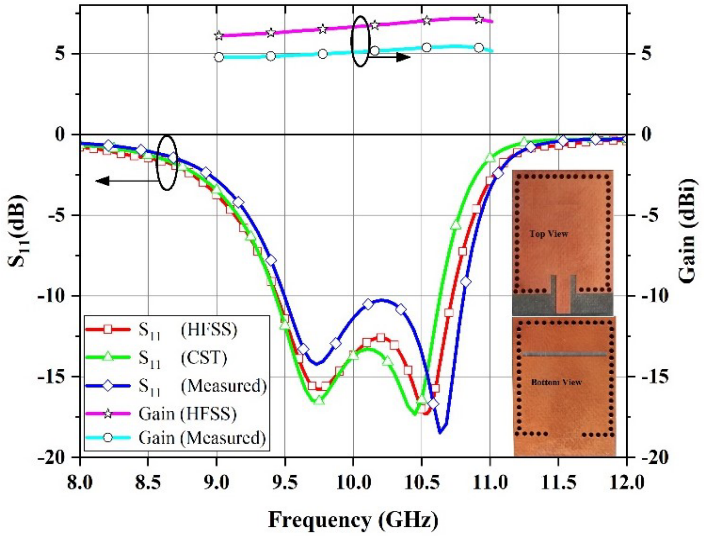

Figure 12. Simulated and measured S_{11} and gains of the antenna.

Anritsu MS2037C network analyzer. Measured and simulated results of the S_{11} and gain confirm the wideband response as plotted in Figure 12. It can be substantiated from the figure that the simulated resonances are 9.75 GHz and 10.5 GHz. The measured ones are 9.73 GHz and 10.63 GHz. The measured impedance bandwidth is 1.3 GHz (12.8%), lying between 9.5 GHz and 10.8 GHz. More information with simulated counterpart is summarized in Table 2. The measured gain versus frequency is included in Figure 12. The antenna exhibits a gain of 6.4 dBi at 9.73 GHz and 7.1 dBi at 10.63 GHz.

The co- and cross-polarization patterns of the designed antenna at two frequencies in two orthogonal planes (XZ-plane ($\phi = 0°$) and YZ-plane ($\phi = 90°$)) are shown in Figure 13. It is obtained with the help of the test antenna in an anechoic chamber. It is found that the far-field patterns at 9.73 GHz and 10.63 GHz are unidirectional and oriented towards the broadside direction. The peak cross-polar levels are -29 dB and -21 dB in the XZ-plane and YZ-plane, respectively at a lower resonance. At 10.63 GHz, they are -34 dB and -20 dB. The front-to-back ratio (FTBR) of the proposed design is about 14 dB and 18 dB respectively at 9.73 GHz and 10.63 GHz. The half-power beamwidths of the

Table 2. Comparison of simulation and measurement results.

Parameter	Simulation (HFSS)	Simulation (CST)	Measurement
f_1, Lower Resonance (GHz)	9.75	9.73	9.73
f_2, Upper Resonance (GHz)	10.5	10.44	10.63
S_{11} (dB) at f_1	−15.82	−16.5	−14.23
S_{11} (dB) at f_2	−17.27	−17.14	−18.46
Impedance Bandwidth (GHz)	9.45 to 10.7	9.43 to 10.63	9.5 to 10.8
FBW (%)	12.4	11.96	12.8

Table 3. Performance comparison: Our work with existing works.

Properties → / References ↓	Year	Freq. band	FBW (%)	Gain (dBi)	Cross-pol (dB)	Structure	h (mm)	ε_r
[12]	2008	X	1.7	5.4	−19	Simple	0.5	2.2
[13]	2012	X	6.3	6	−29	Simple	0.5	2.2
[14]	2013	X	4.2	5.6	−30	Simple	0.787	2.2
[15]	2014	X	9.4	3.7	−18	Complex	0.787	2.2
[16]	2014	Ku	1.66	6.1	NM	Complex	0.787	2.2
[17]	2014	X	8	7.9	−16	Complex	0.787	2.2
[18]	2017	Ku	11	8	−20	Complex	1.57	2.2
[19]	2018	Ku	5.7	6.4	−25	Complex	1.57	2.2
[22]	2019	S	11.9	4.3	NM	Complex	1.57	2.5
[23]	2012	X	8.9	5.2	NM	Complex	0.762	3.48
[24]	2021	X	12.1	6.6	−20	Complex	1.6	2.2
[25]	2020	C	5.2	7.15	−21	Complex	1.524	3.55
[26]	2018	S	3.72	4.42	NM	Complex	1.52	2.5
[27]	2014	X	11.2	8	NM	Complex	1.5	2.55
[28]	2013	X	10.9	7.7	−20	Complex	1.016	2.2
[29]	2012	S	3.71	5	NM	Complex	1.57	2.2
[30]	2012	S	2.16	NM	NM	Complex	2	2.2
Our work	2022	X	12.8	7.1	−34	Simple	1.57	2.2

co-pol pattern in XZ-plane and YZ-plane are about 115° and 74°, respectively, in the lower resonance. Similarly, at 10.63 GHz, they are 114° and 65° in both the planes. To highlight our proposed work, a comparison of different parameters of the proposed design with the previous works are listed in Table 3. It can be observed that our work renders a better bandwidth performance and showcases adaptability in tuning bandwidth. Moreover, the proposed technique can also be applied to SIW based antennas operating at millimetre wave band to have similar performance, which will be addressed in future work.

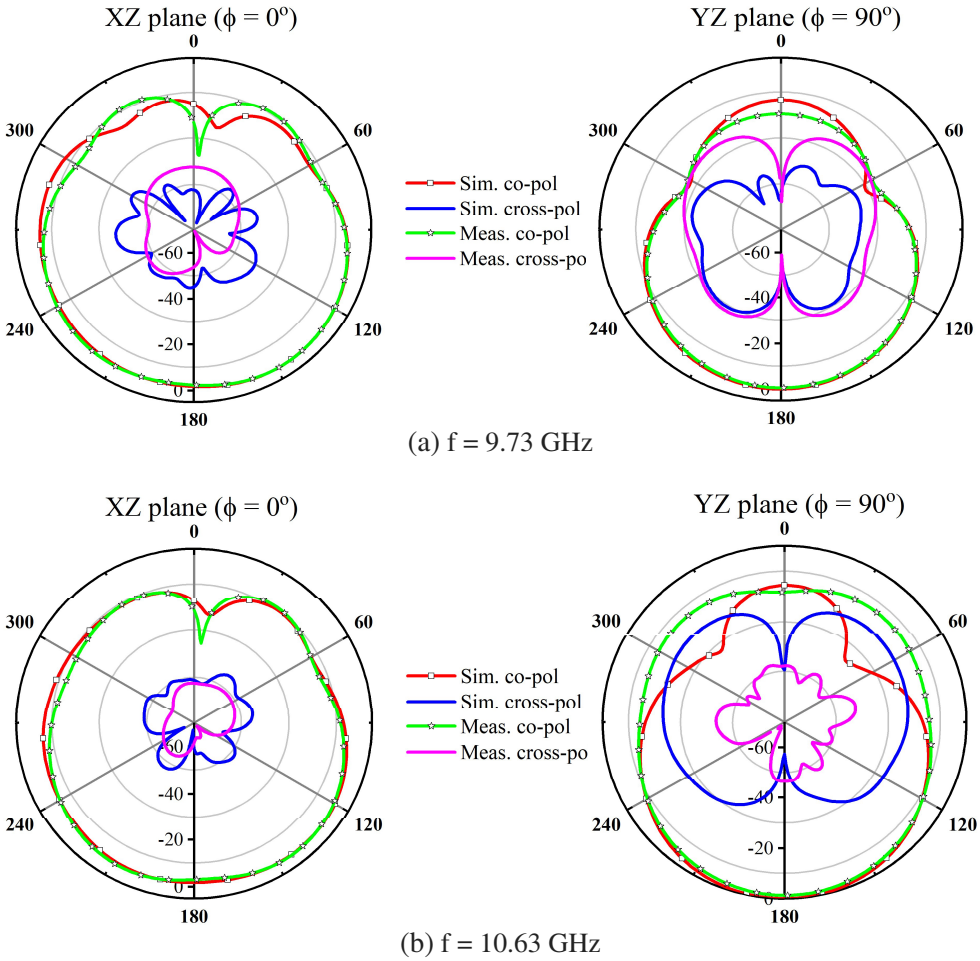

Figure 13. Radiation patterns of the wideband antenna at (a) 9.73 GHz, (b) 10.63 GHz.

6. CONCLUSION

In this article, a bandwidth-enhanced SIW based slot antenna is designed and analyzed. A microstrip line feeding is incorporated into the antenna to excite the SIW cavity. A simple rectangular slot is lodged at the bottom plane for radiating the electromagnetic waves. Subsequently, the TE_{210} mode is apportioned into odd and even TE_{210}, which results in more impedance bandwidth. Circuit models are also developed and have been justified with full-wave simulations. The measured findings show a maximum gain of more than 5 dBi and fractional bandwidth of 12.8%. Good agreement has been achieved between the measured and simulated results. The antenna also possesses benefits, e.g., low profile, light weight, easy fabrication, and high gain.

REFERENCES

1. Yoshimura, Y., "A microstrip slot antenna," *IEEE Trans. Microw. Theory Tech.*, Vol. 20, No. 11, 760–762, 1972, https://10.1109/TMTT.1972.1127868.
2. Lee, Y. C. and J. S. Sun, "Compact printed slot antennas for wireless dual-and multi-band operations," *Progress In Electromagnetics Research*, Vol. 88, 289–305, 2008.

3. Lokeshwar, B., D. Venkatasekhar, and A. Sudhakar, "Quad band substrate integrated waveguide cavity backed slot antenna using balanced shorting vias," *Wireless Pers. Commun.*, Vol. 125, 2565–2579, 2022, https://doi.org/10.1007/s11277-022-09674-2.
4. Harikowa, J., H. Arai, and N. Goto, "Cavity-backed wide slot antenna," *IEE Proceedings H — Microw. Antennas Propag.*, Vol. 136, No. 1, 29–33, 1989, https://doi.org/10.1049/ip-h-2.1989.0005.
5. Basit, M. A., G. Wen, N. Rasool, and X. Xue, "A wide-band cavity-backed slot antenna for end-fire radiation," *Microwave & Optical Tech. Letters*, Vol. 58, No. 1, 193–196, 2016, https://doi.org/10.1002/mop.29524.
6. Deslandes, D. and K. Wu, "Integrated microstrip and rectangular waveguide in planar form," *IEEE Microw Wirele. Comp. Lett.*, Vol. 11, No. 2, 68–70, 2001, https://doi.org/10.1109/7260.914305.
7. Bozzi, M., A. Geordiadis, and K. Wu, "Review of substrate-integrated waveguide circuits and antennas," *IET Microwaves Antennas Propag.*, Vol. 5, No. 8, 909–920, 2011, https://doi.org/10.1049/iet-map.2010.0463.
8. Kumar, A., G. Saini, and S. Singh, "A review on future planar transmission line," *Cogent. Eng.*, Vol. 3, No. 1, 1–12, 2016, https://doi.org/10.1080/23311916.2016.1138920.
9. Uchimura, H., T. Takenoshita, and M. Fujii, "Development of a laminated waveguide," *IEEE Trans. Microw. Theory Tech.*, Vol. 46, No. 12, 2438–2443, 1998, https://doi.org/10.1109/22.739232.
10. Lokeshwar, B., D. Venkatasekhar, and A. Sudhakar, "Wideband low-profile SIW cavity-backed bilateral slots antenna for X-band application," *Progress In Electromagnetics Research M*, Vol. 97, 157–166, 2020.
11. Bollavathi, L., V. Dorai, and S. Alapati, "Wideband planar substrate integrated waveguide cavity-backed amended dumbbell-shaped slot antenna," *AEU — Int. J. of Electron. Commun.*, Vol. 127, 153489, 2020, https://doi.org/10.1016/j.aeue.2020.153489.
12. Luo, G. Q., Z. F. Hu, L. X. Dong, and L. L. Sun, "Planar slot antenna backed by substrate integrated waveguide cavity," *IEEE Antennas Wireless Propag. Lett.*, Vol. 7, 236–239, 2008, https://doi.org/10.1109/LAWP.2008.923023.
13. Luo, G. Q., Z. F. Hu, W. J. Li, X. H. Zhang, L. L. Sun, and J. F. Zheng, "Bandwidth enhanced low-profile cavity-backed slot antenna by using hybrid SIW cavity modes," *IEEE Trans. on Antennas Propagat.*, Vol. 60, 1698–1704, 2012, https://doi.org/10.1109/TAP.2012.2186226.
14. Mukherjee, S., A. Biswas, and K. V. Srivastava, "Bandwidth enhancement of substrate integrated waveguide cavity backed slot antenna by offset feeding technique," *IEEE Appl. Electromagn. Conf.*, 1–2, 2013, https://doi.org/10.1109/AEMC.2013.7045029.
15. Mukherjee, S., A. Biswas, and K. V. Srivastava, "Broadband substrate integrated waveguide cavity-backed bow-tie slot antenna," *IEEE Antennas Wireless Propag. Lett.*, Vol. 13, 1152–1155, 2014, https://doi.org/10.1109/LAWP.2014.2330743.
16. Baghernia, E. and M. H. Neshati, "Development of a broadband substrate integrated waveguide cavity backed slot antenna using perturbation technique," *Appl. Comput. Electromagn. Soc. J.*, Vol. 29, 847–855, 2014.
17. Varnoosfadetrani, M. V., J. Lu, and B. Zhu, "Matching slot role in bandwidth enhancement of SIW cavity-backed slot antenna," *Asia-Pacific Conf. on Antennas and Propag.*, 244–247, 2014, https://doi.org/10.1109/APCAP.2014.6992464.
18. Kumar, A. and S. Raghavan, "Wideband slotted substrate integrated waveguide cavity backed antenna for Ku-band application," *Microwave Opt. Technol. Lett.*, Vol. 59, No. 7, 1613–1619, 2017, https://doi.org/10.1002/mop.30594.
19. Heydarzadeh, F. and M. H. Neshati, "Design and development a wideband SIW based cavity-backed slot antenna using two symmetrical circular corner perturbations," *Int. J. RF Microw. Comput. Aided Eng.*, Vol. 28, No. 9, e21552, 2018, https://doi.org/10.1002/mmce.21552.
20. Dashti, H. and M. H. Neshati, "Development of low profile patch and semi-circular SIW cavity hybrid antennas," *IEEE Trans. Antennas Propag.*, Vol. 62, No. 9, 4481–4488, 2014, https://doi.org/10.1109/TAP.2014.2334708.

21. Sarani, A. V., M. H. Neshati, and M. Fazaelifar, "Development of a wideband hexagonal SIW cavity-backed slot antenna array," *AEU — Int. J. Electron. Commun.*, Vol. 139, 153915, 2021, https://doi.org/10.1016/j.aeue.2021.153915.
22. Niu, B. J. and J. H. Tan, "Bandwidth enhancement of low-profile SIW cavity antenna with bilateral slots," *Progress In Electromagnetics Research Letters*, Vol. 82, 25–32, 2019.
23. Feng, C., J. Yang, L. Yan, Y. Zhang, Y. Geng, and W. Zhang, "Broadband substrate-integrated waveguide slot antenna," *Electromagnetics*, Vol. 32, No. 5, 294–304, 2012, https://doi.org/10.1080/02726343.2012.686844.
24. Lokeshwar, B., D. Venkatasekhar, and A. Sudhakar, "Development of a low-profile broadband cavity backed bow-tie shaped slot antenna in SIW technology," *Progress In Electromagnetics Research Letters*, Vol. 100, 9–17, 2021.
25. Ali, H. A., E. Massoni, L. Silvestri, M. Bozzi, L. Perregrini, and A. Gharsallah, "Increasing the bandwidth of cavity-backed SIW antennas by using stacked cavities," *Int. J. Microw. Wirel. Tech.*, Vol. 10, No. 8, 942–947, 2018, https://doi.org/10.1017/S1759078718000478.
26. Chaturvedi, D., "SIW cavity-backed 24° inclined-slots antenna for ISM band application," *Int. J. RF Microw. Comput. Aided Eng.*, Vol. 30, e22160, 2020, https://doi.org/10.1002/mmce.22160.
27. Liu, L., H. Wang, Z. Zhang, Y. Li, and Z. Feng, "Wideband substrate integrated waveguide cavity-backed spiral shaped patch antenna," *Microw. Opt. Technol. Lett.*, Vol. 57, No. 2, 332–337, 2015, https://doi.org/10.1002/mop.28844.
28. Yang, W. and J. Zhou, "Wideband low profile substrate integrated waveguide cavity backed E-shaped patch antenna," *IEEE Antennas Wireless Propag. Lett.*, Vol. 12, 143–146, 2013, https://doi.org/10.1109/LAWP.2013.2241011.
29. Yun, S., D. Y. Kim, and S. Nam, "Bandwidth enhancement of cavity backed slot antenna using a via-hole above the slot," *IEEE Antennas Wireless Propag. Lett.*, Vol. 11, 1092–1095, 2012, https://doi.org/10.1109/LAWP.2012.2215911.
30. Yun, S., D. Y. Kim, and S. Nam, "Bandwidth and efficiency enhancement of cavity-backed slot antenna using a substrate removal," *IEEE Antennas Wireless Propag. Lett.*, Vol. 11, 1458–1461, 2012, https://doi.org/10.1109/LAWP.2012.2230392.
31. Shi, Y., J. Liu, and Y. Long, "Wideband triple- and quad-resonance substrate integrated waveguide cavity-backed slot antennas with shorting vias," *IEEE Trans. on Antennas Propagat.*, 2017, Vol. 65, No. 11, 5768–5775, https://doi.org/10.1109/TAP.2017.2755118.
32. Wu, Q., J. Yin, C. Yu, H. Wang, and W. Hong, "Broadband planar SIW cavity-backed slot antennas aided by unbalanced shorting vias," *IEEE Antennas Wireless Propag. Lett.*, Vol. 18, No. 2, 363–367, 2019, https://doi.org/10.1109/LAWP.2019.2891108.
33. Lokeshwar, B., D. Venkatasekhar, and A. Sudhakar, "Dual-band low profile SIW cavity-backed antenna by using bilateral slots," *Progress In Electromagnetics Research C*, Vol. 100, 263–273, 2020.